Montaser Bakroon, Reza Daryaei, Daniel Aubram, Frank Rackwitz

Numerical evaluation of buckling in steel pipe piles during vibratory installation

Bakroon, M., Daryaei, R., Aubram, D., & Rackwitz, F. (2019). Numerical evaluation of buckling in steel pipe piles during vibratory installation. Soil Dynamics and Earthquake Engineering, 122, 327–336. https://doi.org/10.1016/j.soildyn.2018.08.003

Numerical evaluation of buckling in steel pipe piles during vibratory installation

Abstract: The buckling of steel pipe piles during installation is numerically studied. Generally, numerical simulation of installation processes is challenging due to large soil deformations. However, by using advanced numerical approaches like Multi-Material Arbitrary Lagrangian-Eulerian (MMALE), such difficulties are mitigated. The Mohr-Coulomb and an elastic-perfectly plastic material model is used for the soil and pile respectively. The pile buckling behavior is verified using analytical solutions. Furthermore, the model is validated by an experiment where a pipe pile is driven into sand using vibratory loading. Several case scenarios, including the effects of heterogeneity in the soil and three imperfection modes (ovality, out-of-straightness, flatness) on the pile buckling are investigated. The numerical model agrees well with the experimental measurements. As a conclusion, when buckling starts, the penetration rate of the pile decreases compared to the non-buckled pile since less energy is dedicated to pile penetration given that it is spent mainly on buckling.

Keywords: Pipe pile buckling, Imperfection, Pile installation, Soil-structure interaction, Multi-Material Arbitrary Lagrangian-Eulerian, Large deformations

1 Introduction

1.1 Motivation

Instability due to buckling is one of the dominant pile failure modes which leads to a sudden increase in pile deformation. Buckling is often observed in slender structures subjected to axial compressive force [1]. The topic of buckling is broad and actively discussed in the field of structural and mechanical engineering. However, the focus of this study is to evaluate pile buckling during installation processes concerning heterogeneity in the soil and pile imperfections. During installation, the pile penetrates the soil which provides to some extent lateral support. Therefore, the embedded part of the pile behaves differently compared to the upper part of the pile which is not yet laterally supported. In most studies of pile buckling, only one of these conditions is assumed, i.e., either a pile with no lateral supports or a completely embedded pile. Hence, the buckling evaluation during installation process under semi-embedded pile condition is the motivation of this study. Semi-embedded piles are frequently observed in offshore geotechnical engineering.

Generally speaking, buckling is classified into two main groups: Global buckling, where the pile deforms in a way similar to Euler's buckling problem, and local buckling, where the pile deformation occurs in the cross-section and is usually localized [2,3].

The global buckling phenomenon is characterized by defining a critical stress/load which depends on the slenderness ratio (Length/radius of gyration) and structure stiffness. Moreover, the critical stress can be considered as a state dividing two types of equilibrium, i.e., before reaching critical stress, the problem is in stable equilibrium, whereas after passing the critical stress, an unstable equilibrium is reached. In geotechnical engineering design codes for pile performance, the general buckling is considered using the slenderness ratio as well as the soil and pile stiffness [3].

The local buckling, on the other hand, is usually characterized as localized damage to the pile which can occur at any stage of pile installation or operation. Local buckling can occur due to several reasons such as pile imperfections, impact with obstacles, forces induced by the soil, etc. Local buckling which is often encountered at the pile tip may cause increased driving resistance, pile deviation from its longitudinal axis which in turn decrease its bearing capacity, and changed pile response to lateral loads due to change in section modulus. By further penetration, the pile may collapse [4]. Also, Chajes [5] reported that a small initial imperfection in a column results in less load-carrying capacity than Euler load.

In practice, one can refer to Rennie and Fried [6] as one of the first works which mentioned and addressed pile buckling during pile installation. Another example of local/pile tip buckling during pile installation is the Goodwyn-A platform construction project in Australia where many piles were severely crushed during installation [7]. It was reported that the major reason for pile collapse was the damage propagation starting from the pile tip. A similar case was observed at Valhall water injection platform where five out of eight skirt piles were damaged during installation [8].

In analytical studies, there are numerous researches regarding pile buckling. Timoshenko and Gere [1] derived empirical solutions to calculate the critical buckling stress for cylindrical shells as well as effects of fabrication inaccuracies. Young et al. [9] listed a comprehensive database of different structural shapes under various loading conditions including cylindrical shells. In another study, Aldridge et al. [4] compared the soil and pile stiffness to consider soil-structure interaction, and concluded that in order to have progressive buckling, the soil must be stiffer than the pile. Otherwise the pile deformation will spring back elastically.
The buckling effect in pile bearing capacity has also been experimentally evaluated. Singer et al. [10] compiled various experiments with their theoretical background on buckling evaluation of thin-walled structures as well as state of the art in experiments. A recent study was also conducted by Vogt et al. [11] where they investigated micropile performance in soft clay. Based on the experimental results, they developed a mathematical model which accounts for soil structure interaction as well as the pile imperfection.

1.2 Previous research in numerical pile buckling analysis

The performance of the numerical simulation of pile buckling can be evaluated from various viewpoints, including simulation of large deformations in the soil, the capability of detecting buckling in a pile during installation, and effect of pile imperfections on driving performance. Geotechnical installation processes, like pile driving and vibro-replacement, generally involve large deformations and material flow which pose simulation challenges when conventional numerical methods are used. Moreover, during the installation process, the pile can be subjected to extreme loads due to soil resistance which induces irreversible deformations to the pile, which results in poor pile performance. Finally, the pile shape may contain imperfections due to fabrication inaccuracies or transportation effects, which causes non-uniform stress distribution and can result in reduced performance.
Numerical methods have been increasingly used in recent decades to study pile buckling problems. These studies can be divided into two groups, namely those done in the field of structural engineering, where the concern is the structural response of the pile, and those done in geotechnical engineering where the soil-structure interaction effects on pile stability are evaluated.
The field of structure buckling, especially the buckling of shell structures, is vast. However, the literature review is limited to studies regarding pipe piles. In a general report done by Schmidt [12], the advances in buckling studies of shell structures including the underlying theory, design code criteria, and use of numerical models are compiled. In the recent decade, several types of research focused on the effects of imperfection in pile strength reduction such as [13–15].
Generally, numerical studies of pile buckling in geotechnical engineering can be categorized according to how soil-structure interaction is taken into account.
A group of numerical models uses a system of non-linear lateral springs to capture the pile confinement due to the soil, which is commonly referred to as “p-y” method. Such methods employ complex equations for springs to capture realistic soil behavior. The “p” term refers to lateral soil pressure per unit length of pile, while the term “y” refers to lateral deflection [16]. The “p-y” method has been used for various geotechnical problems concerning pile buckling, such as evaluation of pile buckling embedded in liquefiable soils [17,18], buckling in partially embedded piles [19,20], and buckling of piles with initial imperfections [21].
Another group of numerical models defines the surrounding soil as elements whose interaction with the pile is defined through a contact model. Most of these models consider structural elements as “wished-in-place,” meaning that the pile installation process has no effect on stress distribution; see for instance [22,23].
This assumption was mostly made to avoid huge mesh distortion issues in numerical simulation of the installation process. The wished-in-place assumption may not be generally realistic with regard to confinement realization of soil presence due to two reasons. First, the soil is disturbed by the installation process, for example, soil densification during hammering. Second, deformations may be induced in a pile during installation, whose effects on the pile bearing capacity is discussed in [24]. Therefore, the wished-in-place assumption can result in an overestimated pile bearing capacity.

Consequently, a new approach is required which can reduce the assumptions made in previous methods. It is believed that numerical approaches specialized for large deformation analysis can be a good candidate for such studies.
In this study, a novel numerical approach is presented which enables studying pile buckling during installation in the soil. By using this method, the complex behavior of soil structure interaction is captured. Various complexities can be taken into consideration such as initial pile imperfection. To the knowledge of the authors, numerical evaluation of buckling behavior of perfect or imperfect piles during installation in soil considering soil-structure interaction has not been studied in literature so far.
The structure of the paper is as follows: in section 2, the developed numerical model is discussed along with the employed material models. The model is then validated using both empirical equations and experimental results. In section 3, a parametric study is conducted to investigate the heterogeneity effect of the soil as well as the effects of initial imperfections in installation performance. Subsequently, the concluding remarks are presented and discussed. In section 4, the results are summarized and discussed. Finally, an outlook for future works is presented.

2 Numerical model

2.1 Description of the MMALE method

Pile installation is considered as a large deformation problem, a group of problems whose numerical analysis via the conventional numerical approaches is often challenging [25–27]. Efforts are made to improve the current available numerical techniques to treat this particular type of problems. Concerning methods that rely on a computational mesh, one of the most promising approaches is the Multi-Material Arbitrary Lagrangian-Eulerian (MMALE) method [28].
The general strategy of MMALE is to generate a mesh usually non-aligned with material boundaries or material interfaces. This may give rise to so-called multi-material elements containing a mixture of two or more materials. A material-free or void mesh zone must be introduced which holds neither mass nor strength. Such zones are necessary for non-Lagrangian calculations to catch material flow into initially unoccupied (i.e., void) regions of the physical space. After performing one or several Lagrangian steps, the mesh is rezoned to its initial configuration to maintain mesh quality (rezoning/remeshing step). A new arbitrary mesh is developed which is different from the initial mesh configuration. Subsequently, the solution is transported from the deformed mesh to the updated/original mesh (remapping/advection step). The sub-steps are not performed in parallel but in a sequential routine using operator-splitting technique. For more information regarding the MMALE, the reader is referred to [28–30].
The MMALE application in geotechnical problems is limited, although it is popular in simulation of the soil in other fields such as an underground explosion, where the soil is considered as a medium for transmitting shock waves [31]. A recent study conducted by Bakroon et al. [32] assessed the feasibility of MMALE in realistic geotechnical large deformation problems in comparison with classical Lagrangian methods. It was concluded that MMALE could be considered as promising candidates for solving complex large deforming problems. The applicability of MMALE in conjunction with a complex soil material model was also investigated in another work done by Bakroon et al. [33].

2.2 Description of the model

In this section, a description of modeling considerations using MMALE technique in LS-DYNA/Explicit is presented. A model is developed, where a pile is installed in the soil using vibratory force. All the models in the following sections use the same configurations discussed here.
The model configurations in isometric, side, and planar view are shown in Fig. 1 (a-c), respectively. The load history curve of the vibratory force is depicted in Fig. 1d.
The pile has 1.5 m height, 0.2 m diameter, and 0.005 m thickness which is modeled using the conventional Lagrangian element formulation with reduced integration point and a uniform element size of 2-cm (3000 elements). An elastic-perfectly plastic material model based on von Mises failure criterion is used for the pile with properties listed in *Table 1*. A mesh with 2 m height and 1 m radius with the one-point integration MMALE element formulation is generated. A gradient mesh, ranging from 0.6 – 8 cm

element width is used in the horizontal direction, whereas a uniform mesh in the vertical direction with 2.5 cm is considered (367,200 elements). The mesh is filled with the soil up to the height of 1.8 m. A void domain with 0.2 m height, which has neither mass nor strength, is defined above the soil material to enable the soil to move to this domain after penetration starts. To avoid additional complexities regarding the soil material model, the Mohr-Coulomb constitutive equation is adopted, whose corresponding material constants for Berlin sand are estimated and listed in
Table 2. The initial stress in the soil is defined with assigning the gravity acceleration as 10 m/s^2.
The equipotential smoothing technique is applied where the computational grids are rearranged to maintain the mesh quality [34]. For the advection step, the 2nd-order accurate van Leer method is chosen [35].
For installation processes, the pile is characterized by using the Lagrangian formulation whereas the soil in MMALE is defined by using the Eulerian formulation. Coupling thus becomes necessary between the Lagrangian and Eulerian meshes. To define the coupling between pile and soil, penalty contact is defined with a tangential friction coefficient of 0.1. The pile head is fixed against horizontal movements. The lateral sides of the soil are constrained against movements in a direction perpendicular to their faces, while fixity in all directions is applied to the bottom of the soil.
The process of numerical model validation is presented which is divided into two main parts, verification of the pile element formulation, and validation against experimental results. The first part focuses mainly on differences in results obtained from the shell and solid element formulation using three benchmark tests to achieve a realistic pile behavior. The second part deals with the soil-structure interaction model as well as the performance of MMALE by comparing to experimental measurements.

Table 1 General properties of the pile used in benchmark models

Density ρ (kg/m^3)	Elastic Modulus E (MPa)	Yield Stress σ_y (MPa)	Poisson ratio υ	Thickness t (m)	Radius R (m)
7850	2.1E5	250	0.3	0.005	0.1

Table 2 Mohr-Coulomb material constants for Berlin sand [36]

Density ρ (kg/m^3)	Friction angle ϕ	Dilatancy angle ψ	Cohesion c (MPa)	Poisson ratio υ	Elastic Modulus E (MPa)
1900	35°	1°	0.001	0.2	20

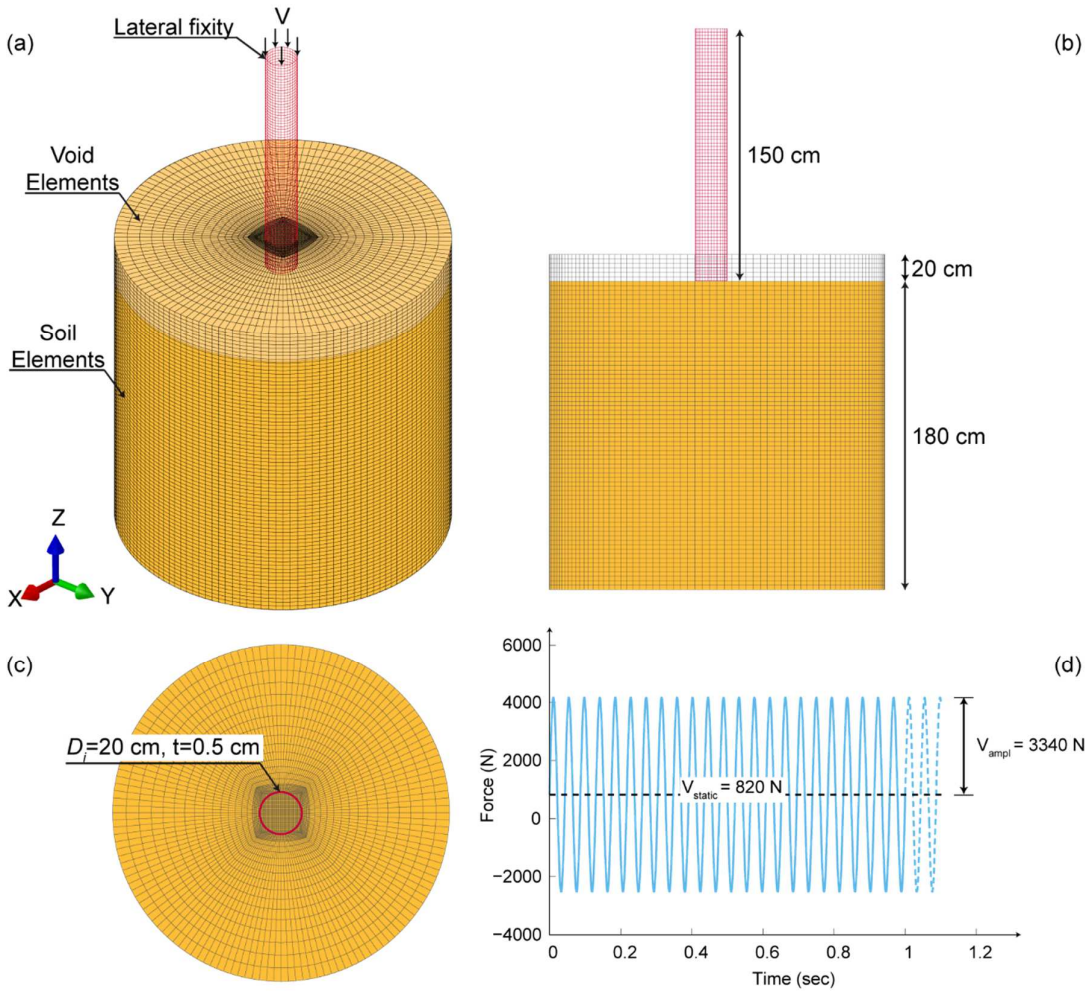

Fig. 1. Schematic diagram of the (a) isometric view, (b) side view, (c) planar view of the one-quarter numerical model configuration with (d) vibratory load history curve

2.3 Verification of shell element formulation

The pile behavior in the numerical model depends on various parameters including the element formulation (shell or solid element), mesh size, and a number of integration points (reduced or full integration). A benchmark model is chosen to evaluate the pile behavior under uniform axial compression. Both solid and shell elements with reduced integration are used. A full integration shell element is also used for comparison. The pile has the properties listed in *Table 1*.

This benchmark model investigates one of the possible forms of buckling in cylindrical pipe piles which occurs due to an applied uniform axial load. Theoretically, the critical uniform axial stress value which causes buckling, σ_{cr}, is calculated by Timoshenko and Gere [1]:

$$\sigma_{cr} = \frac{E\,t}{R\sqrt{3(1-\nu^2)}} \tag{1}$$

A numerical model is developed to evaluate the axial critical stress using different element formulations. The model configuration is shown in Fig. 2. A pile with a length of 0.25 m is generated which is under a distributed axial compressive load with a total magnitude of 100 KN. It should be noted that this load does not play a role in eigenvalue calculation and is only used to show the load application direction.

Initially, a mesh size of 0.005 m is chosen which provides reasonably accurate results. The pile is fixed in the bottom while the top surface is fixed in horizontal directions (X and Y).

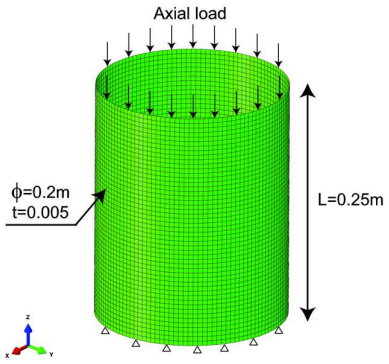

Fig. 2. Benchmark model configuration under uniform axial compression

The comparison criterion is the least eigenvalue which is subsequently used to calculate the critical buckling stress. The corresponding critical stress is compared with the empirical Eq. (1). The buckling mode determined from each element formulation is shown in Fig. 3. as well as their corresponding eigenvalues and critical axial stress as listed in Table 3. The shell elements provide an accurate result with about 5% difference while the solid element significantly underestimated the critical buckling stress compared to the empirical equation. The difference between reduced and full integration shell element is negligible.

Table 3 Comparison of the resulting critical buckling stress under axial pressure

	Eigenvalue	Critical stress (MPa)
Empirical equation [1]	199.6	6.35E3
Reduced integration shell	189.4	6.03E3
Full integration shell	189.2	6.02E3
Reduced integration solid	20.1	0.64E3

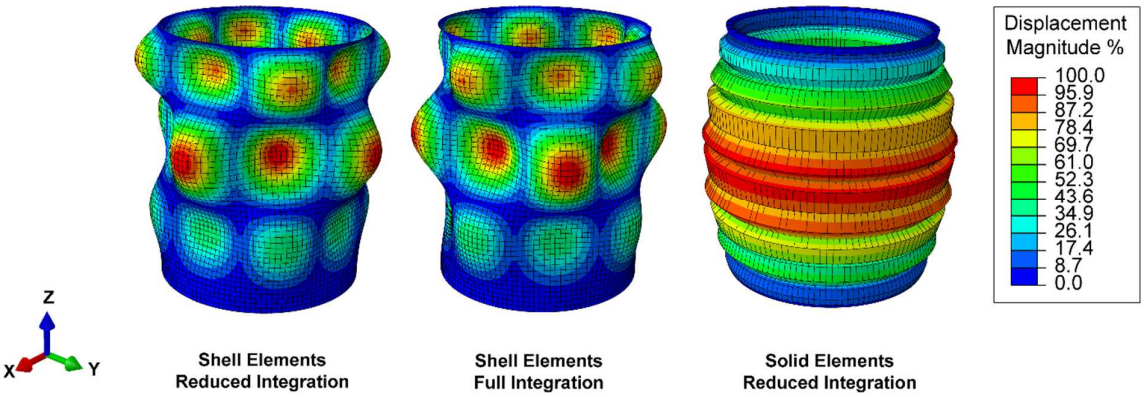

Fig. 3. Resulting buckling modes using different element formulations.

2.4 Validation against experimental results

The proposed numerical model is validated by back-calculating an experimental test carried out at the laboratory of the Chair of Soil Mechanics and Geotechnical Engineering at Technische Universität Berlin (TU Berlin). The test set-up consists of a half-cylindrical pile with 1.5 m length, 0.005 m thickness, and 0.2 m outer diameter as well as a chamber with three rigid steel walls and one glass panel. The pile

is fixed in the horizontal direction via pile guides to ensure penetration along the glass panel. A vibratory motor produces the driving force of 1670 N with the frequency of 23 Hz. The imposed dead load on the pile is about 410 N. The chamber is filled with Berlin sand. Two displacement sensors are mounted on the pile to measure vertical pile displacement.

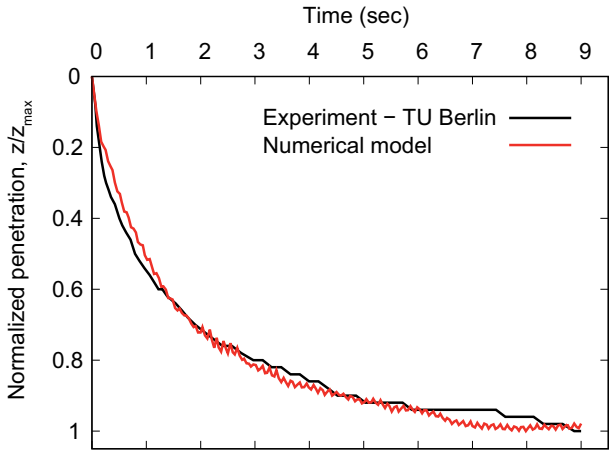

Fig. 4. Penetration depth vs. time curve obtained from the numerical model and experimental measurement

A quarter model is developed based on the descriptions in Section 2.2. Here, to make the model independent of pile properties, the pile is modeled as rigid. Fig. 4 shows the resulting displacement curve obtained from the numerical model compared with experimental measurement. To focus on the evaluation of the penetration trend, the penetration depth is normalized by its maximum value. Initially, the penetration rate is significant due to less soil resistance and confining pressure. By further penetration, the resulting force normal to the pile skin increases considerably, leading to an increase of the frictional force. Therefore, the penetration rate decreases. The same trend was observed in the experiment. Hence, the numerical model captures the penetration trend accurately enough.
Fig. 5 shows vertical and horizontal stress contours at the last compression force cycle of the vibratory loading curve. The contours can be used to determine the size of the influenced area. By evaluating the vertical stress distribution contours (Fig. 5a), it can be observed that the areas around the pile are influenced and disturbed during the installation. A relatively large vertical stress is seen in the soil under the pile tip. At a depth of about 1.3 m from the soil surface, the contours become almost linear, indicating the vibratory force influence region which is reasonably far from the boundary. The horizontal stress as shown in Fig. 5b is relatively large around the pile. In areas far enough from the pile, the lateral stress in the soil reaches its *in-situ* value, which verifies that the boundary distance is far enough from the dynamic source to have substantial effects. Based on the above arguments, it can be said that the numerical model captures the expected behavior of the soil during the pile penetration reasonably.

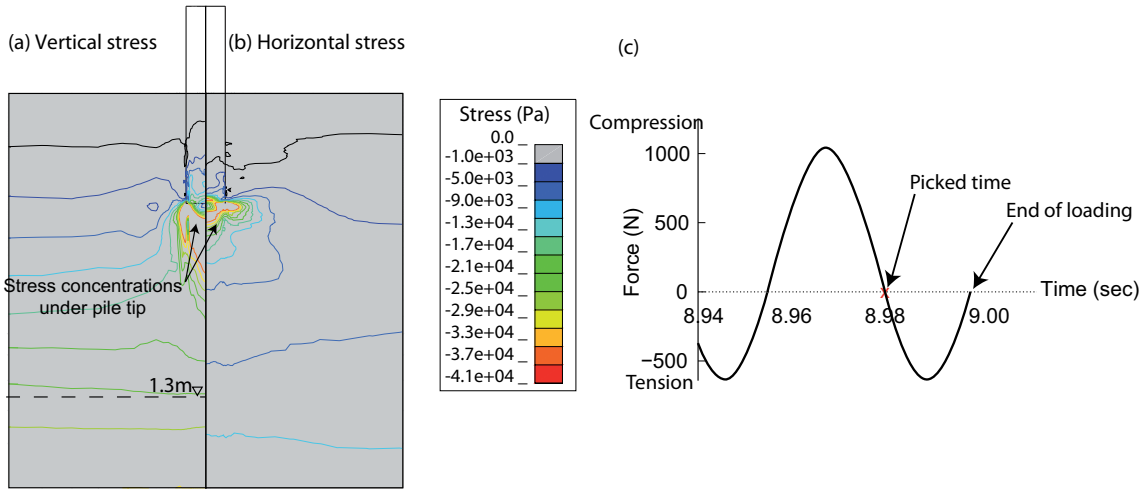

Fig. 5. Isolines of the induced (a) vertical and (b) horizontal stress in the soil, and (c) the corresponding loading at 8.98 sec for the validation model

3 Parametric study of pile buckling during penetration

In this section, the pile buckling phenomenon during installation is evaluated by using the MMALE computational model described in Sect. 2.2. In section 0, a reference model is developed as a comparison basis. In section 3.2, the buckling phenomenon is studied under two distinct conditions, various imperfect piles, and heterogeneous soil. In section 3.3, the results are presented and discussed.

The pile in both the experiment and the numerical model, did not exhibit buckling for this amount of penetration, using realistic parameters. Therefore, in order to reach significant buckling in this small container after a short amount of penetration a low elastic modulus was assigned to the pile. By using a relatively less elastic modulus, a larger calculation time step was also reached in the numerical model. The reduced elastic modulus of the pile is listed in Table 4, which corresponds to 1% of the elastic modulus used in the model in section 2.2. In all the calculations, the harmonic vertical force applied to the pile head is drawn in Fig. 1c.

Table 4 Elastoplastic properties of the pile used in a parametric study

Density ρ (kg/m^3)	Elastic Modulus E (MPa)	Yield Stress σ_y (MPa)	Poisson ratio υ
7850	2.1E3	250	0.3

The models presented in this study, are small scale, compared to the problem size encountered in practice. The reason behind choosing this model dimension was due to the experiment container size, with which the numerical model was validated. In the parametric study, the numerical model is still maintained to avoid modifications in any part of the model. For instance, by scaling up the model size, one has to assign a new loading magnitude.
Nevertheless, it is possible to expand the numerical model to adapt to practical geotechnical applications using realistic values for both soil and pile. To this extent, the model should be scaled up. To do so, one can use larger element sizes while keeping their aspect ratio.

3.1 Reference model

In this model, a perfect cylindrical pile is installed in the soil using a vibratory load. This model is developed as a comparison basis to the models where the pile holds initial imperfection or the soil contains heterogeneity. The comparison criteria are the mean strain, internal energy, load-penetration

curve, and pile lateral displacement. The mean strain is calculated as one-third of the strain tensor trace and defined based on the infinitesimal theory. The internal energy is the work done to induce strain in a unit volume of the solid part which can be used here to evaluate the accumulated strain in a pile during installation. The lateral displacement curve is obtained by averaging the nodal displacements of all nodes in the pile.

With the same model configuration of section 2.2, the pile did not suffer any significant buckling until about 8 seconds of the simulation which corresponds to 0.65 m penetration. Therefore, all the models with imperfections and soil heterogeneity are compared for this duration.

The mean strain contour plots, as well as the deformed pile tip section, are shown in Fig. 6. It is observed that the induced strain in a pile is less than 0.05% which is negligible. Also, the pile tip holds its initial cross-section with minimal deformations. Fig. 7 shows the horizontal stress distribution in the soil at the final stage. The stress contours are almost symmetric, yet different of what was observed in the validation model in Fig. 5. The underlying reason is believed to be caused by the applied changes in the pile, i.e. change of the pile property from a rigid to an elasto-plastic behavior and reduction of its Young's modulus.

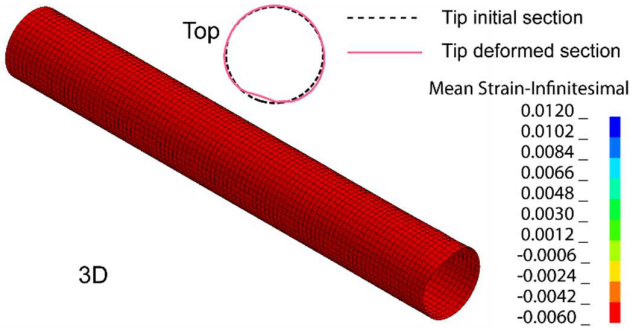

Fig. 6. Mean strain contour plots in pile after 0.65 m penetration for the reference model

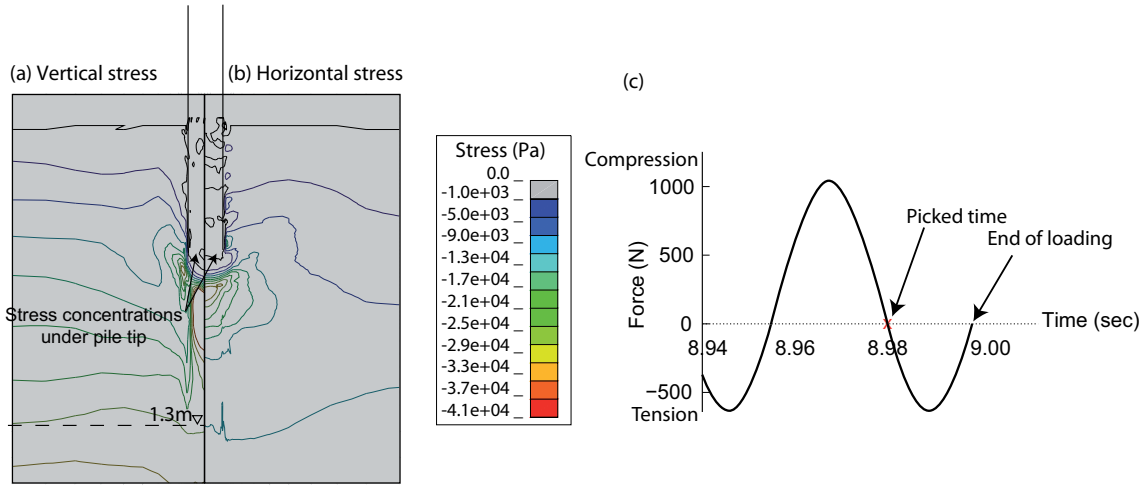

Fig. 7. Isolines of the induced (a) vertical and (b) horizontal stress in the soil, and (c) the corresponding loading at 8.98 sec for the reference model

3.2 Effect of pile imperfection and soil heterogeneity

Initial imperfections are somewhat unavoidable in piles which may have been caused by fabrication tolerances or mishandling in transportation [37]. Although small, the imperfection cannot be neglected since it is proved to have an influence on pile buckling [38]. Currently, a handful of considerations are

available in design codes for the imperfections based on fabrication tolerance [3,39]. The codes are mainly based on empirical equations which don't usually capture the complex condition of installation process which is encountered in practice. The numerical models studied above considered an initially perfect circular section with no imperfections.

To evaluate the imperfection effects on the pile performance, three models are proposed where the pile is modeled initially as imperfect. These include piles with the oval cross-section, flat side, and with out-of-straightness in length. In the following subsections, the characteristics of each imperfection are described. Subsequently, the results from each model are compared and discussed.

3.2.1 Scenario 1: Oval-shaped pile

One of the most common types of imperfection in cylindrical steel pipe piles is Ellipticity/out-of-circularity where the pile takes the shape of an oval. The schematic diagram of an oval-shaped pile compared to a perfect circular pile is shown in Fig. 8. In comparison to a circle, an oval-shaped pile may buckle more during penetration. According to Timoshenko [40], ovality is defined as $w_0 = (D_{max} - D_{min})/4$, where D_{max} and D_{min} correspond to the longest and shortest oval diameter, respectively.
To investigate ovality effects on buckling, a model is developed where an initial out-of-circularity is applied to the pile. The oval pile properties are listed in Table 5.

Table 5 Properties of the oval pile section

D_{max} (cm)	D_{min} (cm)	w_0 (cm) Timoshenko
19.8	18.4	0.35

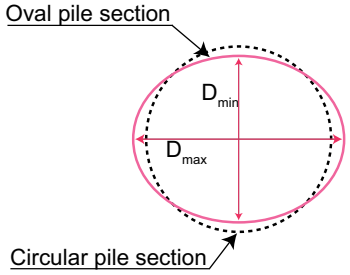

Fig. 8. Schematic diagram of initial pile section compared to a perfect circle

3.2.2 Scenario 2: Out-of-straightness pile

Another form of imperfection is out-of-straightness where the pile top and bottom axis are not on the same vertical axis. This shift in cross-section over length causes different behavior in soil compared to the straight pile. In case of this imperfection, more pressure can be induced on neighboring soil regime since the pile tends to push the soil further to the side. Therefore, the pile can be prone to buckling due to the unbalanced state.
The schematic diagram of this imperfection is shown in Fig. 9 where the pile alignment with respect to the vertical axis differs by the amount of δ. The reduction is applied gradually, starting from the pile head to its tip. The assigned values δ for this model is 1.2 cm.

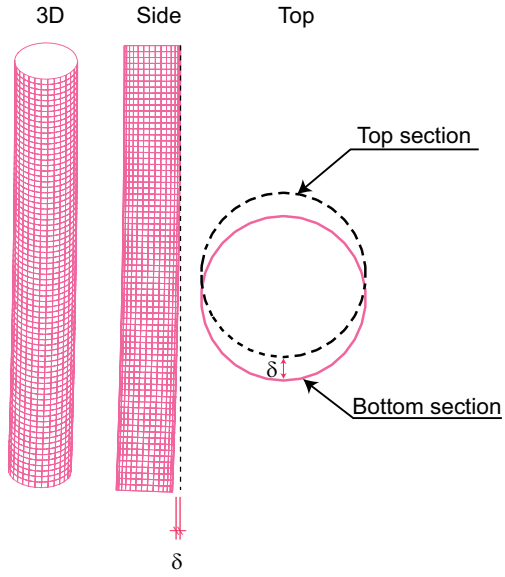

Fig. 9. Schematic of initial pile geometry from different views which illustrates the out-of-straightness

3.2.3 Scenario 3: Flat Pile

This form of imperfection is also common which can be caused during transportation or storage. From the cross-section view, the pile section is deformed, and a part of the curvature is flattened. Fig. 10 shows an example of a pile of flatness. The flatness is defined by two parameters, out-of-roundness, λ, and flatness, c. The parameters c and λ can be related to each other by the following formula, $c = 2\sqrt{\lambda D}$ [39]. A model is developed where the flatness value of c= 7.8 cm is assigned which corresponds to λ= 0.8 cm.

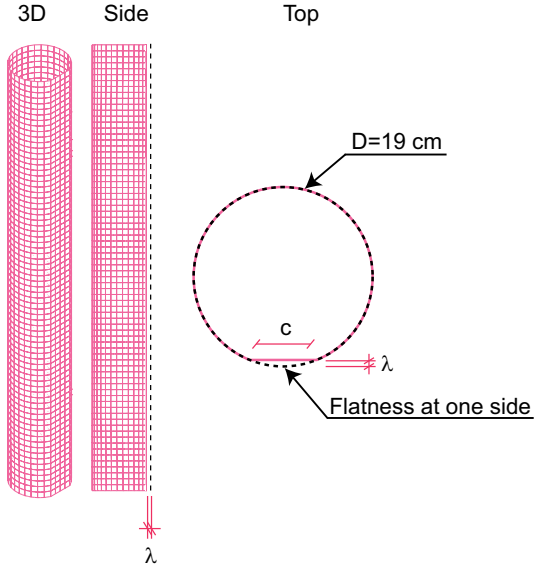

Fig. 10. Schematic diagram of initial pile geometry from different views illustrating flatness

3.2.4 Scenario 4: Heterogeneous soil

In this section, a model is presented, where the pile hits a rigid sphere which somewhat represents a heterogeneity in the soil. This condition which in practice can represent a boulder in the soil, can cause early buckling in a pile and thus affecting its performance during installation. This concept is not rare

in the literature. A similar study was conducted by Holeyman et al. [41] where a Boulder-soil-pile model was simulated using 1-D wave equation theory to study soil and boulder failure mechanisms. The goal of the following model is to study the buckling propagation in a pile with further penetration in the soil after it hits the boulder. The rigid sphere with an assumed diameter of 10 cm is located inside the soil at a depth of 25 cm below the soil surface and 8 cm away from the center of the pile (see Fig. 11). The sphere is assumed fixed in all directions to avoid any extra effects which can be induced by the soil - boulder interaction.

Several further conditions can be included in the model such as the definition of a non-rigid heterogeneity with/without a different geometry. This, however, introduces additional complexities to the model which is not the focus of this study.

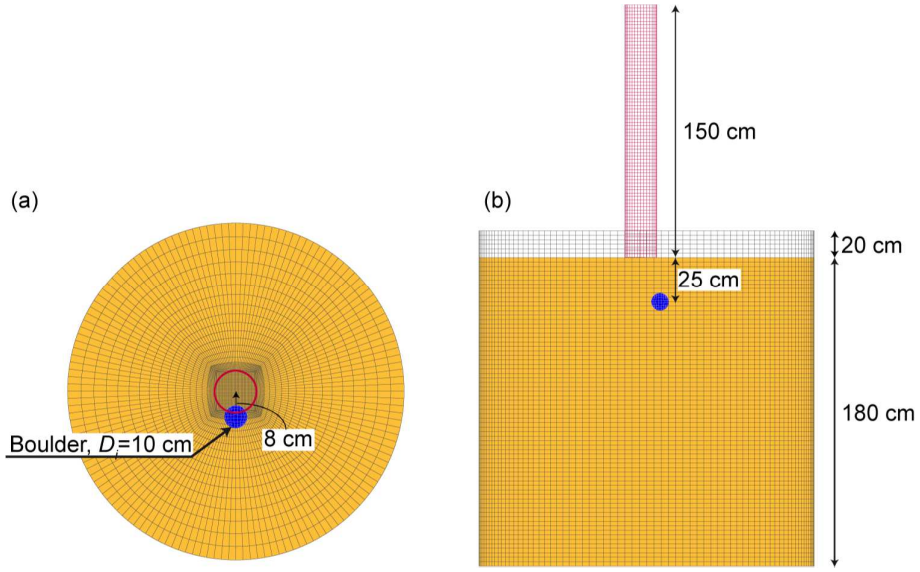

Fig. 11. (a) The planar view and (b) the cross section of the model illustrating the location of the applied heterogeneity (rigid sphere) in the soil

3.3 Results and discussion

3.3.1 Results

The four models (ovality, flatness, straightness, and heterogeneity) are compared in Fig. 12 to the reference model using the criteria mentioned in the previous section. First, the penetration rate of the models is investigated. The reference model penetrated 0.65 m without suffering any significant strain. For the four scenarios, the final penetration is less than the reference model. In case of heterogeneity, the penetration rate decreases after it hits the boulder at 1.5 seconds. After about 2 seconds, the penetration rate of the model with an oval cross-section starts to decrease. The penetration rate of the other two imperfect piles, namely the piles with flatness side and out-of-straightness, decrease after about 4 seconds.
Concerning the fact that the same driving force was used for all models, it can be concluded that the same energy is applied to all the piles. Therefore, according to the energy conservation law, the driving energy must have been spent on other phenomena such as lateral displacements, additional strains and/or buckling in a pile. Therefore, to assess this point, the lateral displacement, as well as the internal energy of each pile, is compared in Fig. 12b and Fig. 12c, respectively.
It is observed that at the same time when the penetration curve differs from the reference model, the corresponding lateral displacement and internal energy of the piles start to increase drastically. The lateral displacement of the pile is limited and is maintained after a specific amount of penetration, which can be attributed to the strong soil resistance. Thus, the remaining driving energy must have been spent on buckling. By comparing Fig. 12b and Fig. 12c, this point becomes clear where after the lateral displacement reaches an almost constant value, the internal energy starts to grow significantly. The curves in Fig. 12c are cut to the value of 42 J. Also, a decrease in the internal energy value is observed after

significant jumps for some models. This can be attributed to the induced elastic strains in the pile which after further penetration the pile springs back elastically. The possibility of the occurrence of this behavior has also been reported by Aldridge et al. [4]. As a result, it can be argued that the driving energy for the pile installation is reflected in the model mainly in three different forms, lateral and horizontal displacement, and pile buckling.

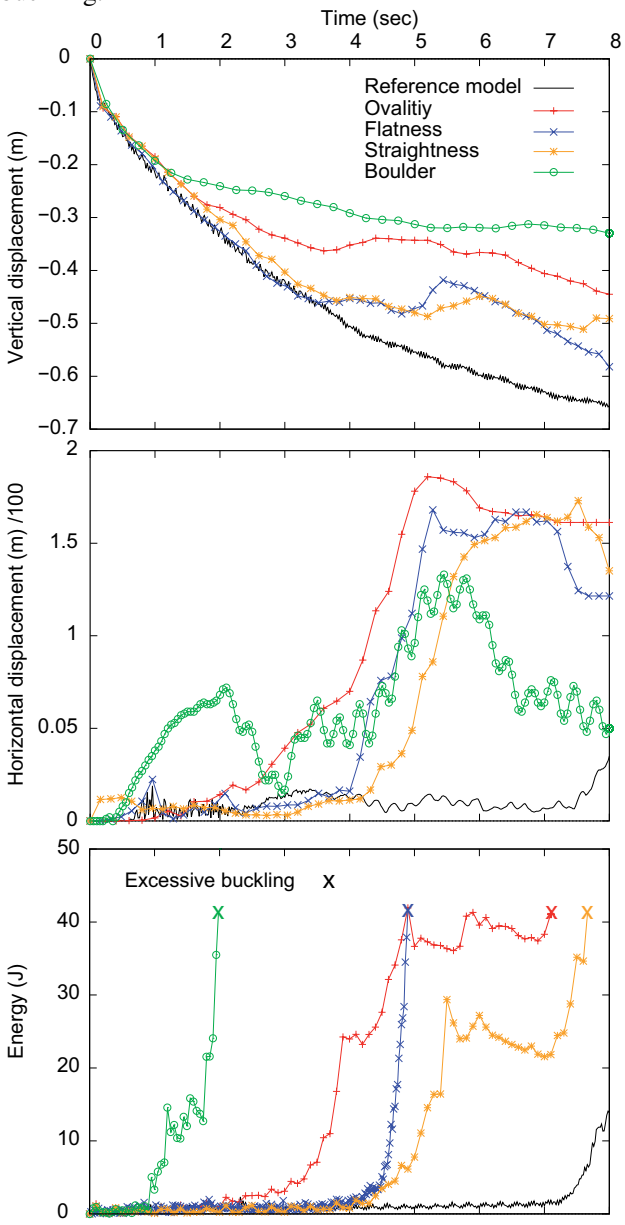

Fig. 12. Comparison of the imperfect piles with the reference model based on the (a) vertical displacement (b) lateral displacement, and (c) the internal energy

The induced mean infinitesimal strain which is defined as one-third of the strain tensor trace, as well as the pile section deformation, are shown for each pile in Fig. 13. The pile shapes correspond to the time stamps, where maximum internal energy was recorded. In comparison to the reference model, a relatively significant strain/buckling is sustained by the piles in the models. Most of the strain is accumulated at the pile tip which points out the damage starting point. Furthermore, the progressive pile deformation after further penetration is non-symmetric. In addition, each model exhibits a different buckling mode due to the different initial imperfection. Also, it is observed that the cross sections of the imperfect piles tend to take the forms similar to the so-called “peanut-shape” as reported in the literature [4,7].

Concerning the above discussion, it is argued that the proposed numerical model captures the complex site conditions such as the effect of soil resistance, pile imperfection, and heterogeneity during installation processes. In addition, the model provides reliable measures to assess pile buckling

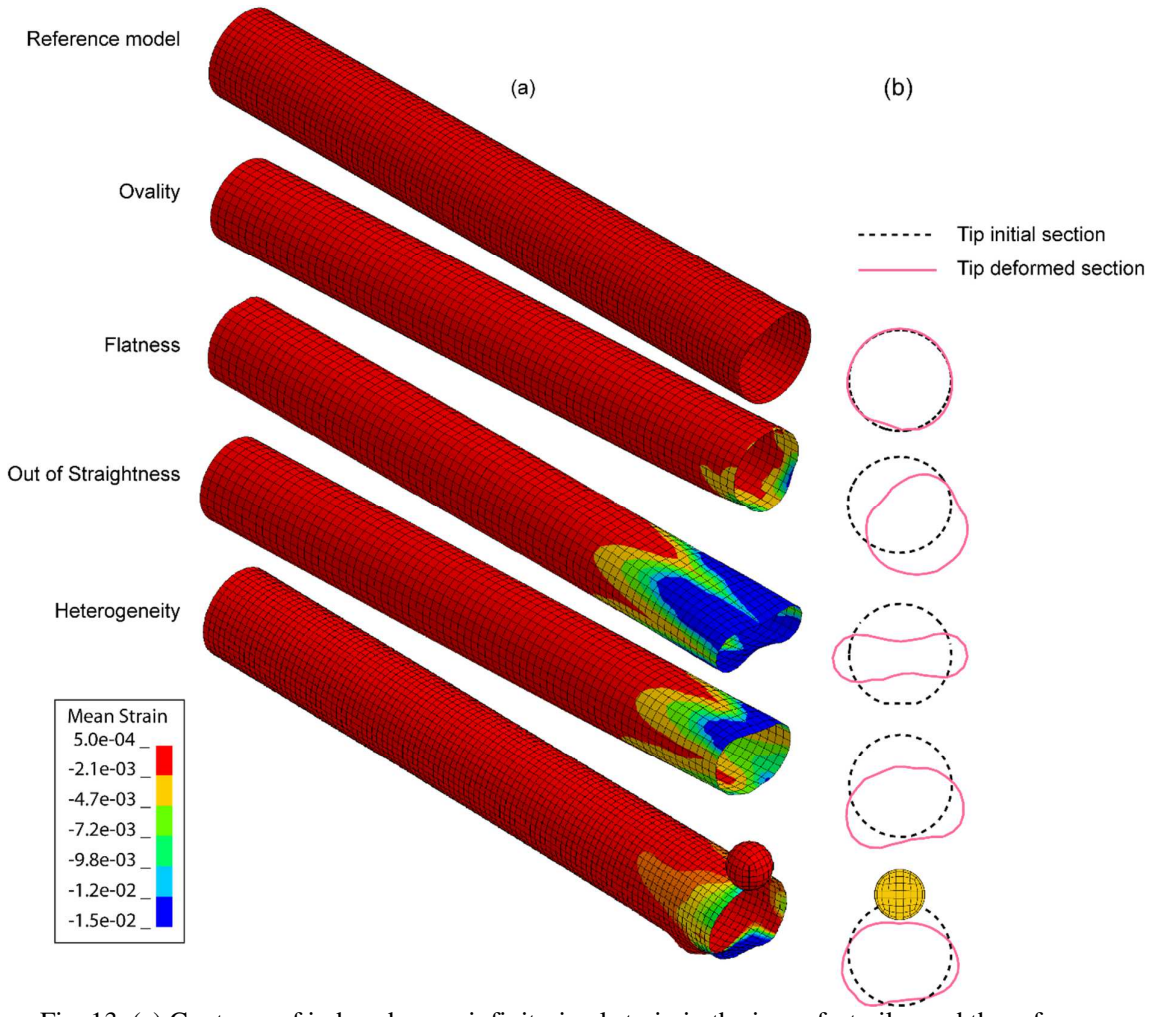

Fig. 13. (a) Contours of induced mean infinitesimal strain in the imperfect piles and the reference model and (b) the pile tip cross section compared to its initial

3.3.2 A brief discussion regarding plugging

In examples above, the soil inside the pile moved as a block along with pile as it was driven. This phenomenon is referred to as plugging which closely affects the pile bearing capacity and also the installation performance. To determine the plugging occurrence and its effect on pile penetration resistance, there are several equations available in the literature [42]. For instance, Jardine et al. [43] derived two equations based on the inner pile diameter, d, CPT tip resistance, $q_{c,a}$, and relative density of the soil, D_r, to determine if plugging occurs:

$$d \geq 2.0(D_r - 0.3) \text{ or } d \geq 0.03 q_{c,a} \quad (2)$$

If one of the two equations is fulfilled, the pile is considered unplugged.
In the current numerical model and the experiment, the corresponding values of D_r and $q_{c,a}$ for Berlin sand are estimated to be 0.75 and 6.3 MPa, respectively [44]. Hence, by having d=0.19 m, none of the conditions above are satisfied, indicating that the plugging may occur during the pile penetration. In both the numerical model and the experiment, plugging was observed. Nevertheless, the plugging is a wide area of research, and therefore it requires further and more focused investigations.

4 Conclusions and outlook

The focus of this study is to evaluate pile buckling during installation processes concerning heterogeneity in the soil and pile imperfections. A novel MMALE numerical approach, with an efficient soil-structure interaction scheme, was employed to improve the numerical analysis of pile buckling which omits simplifications used in previous studies. To capture a realistic buckling behavior of the pile, shell element types with reduced integration points were used which provided a more accurate result than solid elements.

It was observed that the pile rigidity and stiffness play an important role in soil stress distribution during installation. In case of a rigid pile, the stress distribution was different than what was observed in the elasto-plastic pile. The underlying reason can be the pile deformation during the installation. This highlight the importance of consideration of pile deformation during the installation.

In addition, effects of various complex conditions, imperfections in pile geometry and heterogeneities in the soil, were investigated and compared to a reference model where the pile holds perfect cylindrical shape with no heterogeneity in the soil. Each scenario exhibited a different buckling mode. Before a significant buckling could be observed, the penetration rate started to decrease. At this time, both lateral displacement and internal energy started to grow. The outcomes of this work show that the driving energy of pile installation can be spent on other phenomena such as pile buckling and lateral soil displacement. Consequently, less penetration will be observed. In addition, the initial imperfection not only accelerates the buckling process but also changes the buckling mode of the pile.

Although a small-scale model was employed in this study, the proposed numerical approach can be used in large-scale problems. Hence, this approach can help engineers to study the sensitivity of numerous variables, such as pile thickness, diameter, and/or different soil conditions in reaching a cost-effective pile design without encountering buckling during the installation process.

The presented work focused on a specific area, i.e. pile imperfection and soil heterogeneity. There are numerous affecting parameters on pile buckling which cannot be summarized in one study. Following points may also be considered in future works:

- A more realistic soil material model taking into account the various drainage conditions
- Possible effects of various dynamic loading types (hammer or vibratory) using suitable shock-absorbing boundaries
- Soil heterogeneity such as the presence of a lens or multiple layers
- Pile bearing capacity evaluation considering phenomena such as plugging

5 Acknowledgments

The authors are thankful for the partial financial support obtained from German Academic Exchange Service (DAAD) with grant number 91561676.

References

[1] Timoshenko SP, Gere JM. Theory of Elastic Stability. 2nd ed. Michigan: McGraw-Hill; 1961.

[2] Bhattacharya S, Carrington TM, Aldridge TR. Buckling considerations in pile design. Frontiers in Offshore Geotechnics: ISFOG 2005, London: Taylor & Francis Group; 2005, p. 815–21.

[3] DIN EN 1993-1-6:2007. Design of steel structures - Part 1-6: Strength and stability of shell structures. Eurocode 3. 2007.

[4] Aldridge TR, Carrington TM, Kee NR. Propagation of pile tip damage during installation. Frontiers in Offshore Geotechnics, ISFOG 2005 - Proceedings of the 1st International Symposium on Frontiers in Offshore Geotechnics 2005:823–7. doi:10.1201/NOE0415390637.ch94.

[5] Chajes A. Principles of Structural Stability Theory. illustrate. Prospect Heights, IL: Waveland Press; 1974.

[6] Rennie IA, Fried PA. An Account Of The Piling Problems Encountered And The Innovative Solutions Devised During The Installation Of The MAUI "A" Tower In New Zealand. Offshore Technology Conference, Houston, Texas, U.S.A.: Offshore Technology Conference; 1979, p. 723–36. doi:10.4043/3442-MS.

[7] Kramer G. Investigation of the Collapse Mechanism of Open Ended Piles during Installation. TU Delft, 1996.

[8] Alm T, Snell RO, Hampson KM, Olaussen A. Design and Installation of the Valhall Piggyback Structures. Offshore Technology Conference, Houston, Texas, U.S.A.: 2004, p. 1–7.

[9] Young WC, Budynas RG, Roark RJ. Roark's Formulas for Stress and Strain. vol. 43. 7th ed. New York: McGraw-Hill; 2002.

[10] Singer J, Arbocz J, Weller T. Buckling Experiments: Experimental Methods in Buckling of Thin-Walled Structures. vol. 2. Hoboken, NJ, USA: John Wiley & Sons, Inc.; 2002. doi:10.1002/9780470172995.

[11] Vogt N, Vogt S, Kellner C. Buckling of slender piles in soft soils. Bautechnik 2009;86:98–112. doi:10.1002/bate.200910046.

[12] Schmidt H. Stability of steel shell structures. Journal of Constructional Steel Research 2000;55:159–81. doi:10.1016/S0143-974X(99)00084-X.

[13] Hilburger MW, Nemeth MP, Starnes JH. Shell Buckling Design Criteria Based on Manufacturing Imperfection Signatures. AIAA Journal 2006;44:654–63. doi:10.2514/1.5429.

[14] Edlund BLO. Buckling of metallic shells: Buckling and postbuckling behaviour of isotropic shells, especially cylinders. Structural Control and Health Monitoring 2007;14:693–713. doi:10.1002/stc.202.

[15] Ning X, Pellegrino S. Imperfection-insensitive axially loaded thin cylindrical shells. International Journal of Solids and Structures 2015;62:39–51. doi:10.1016/j.ijsolstr.2014.12.030.

[16] API. Recommended Practice for Planning, Designing and Constructing Fixed Offshore Platforms - Working Stress Design. vol. 2A-WSD. 21st ed. Washington: API Publishing Services; 2003. doi:10.1007/s13398-014-0173-7.2.

[17] Bhattacharya S, Adhikari S, Alexander NA. A simplified method for unified buckling and free vibration analysis of pile-supported structures in seismically liquefiable soils. Soil Dynamics and Earthquake Engineering 2009;29:1220–35. doi:10.1016/j.soildyn.2009.01.006.

[18] Dash SR, Bhattacharya S, Blakeborough A. Bending–buckling interaction as a failure mechanism of piles in liquefiable soils. Soil Dynamics and Earthquake Engineering 2010;30:32–9. doi:10.1016/j.soildyn.2009.08.002.

[19] Budkowska BB, Szymczak C. Initial post-buckling behavior of piles partially embedded in soil. Computers & Structures 1997;62:831–5. doi:10.1016/S0045-7949(96)00302-1.

[20] Zhou X-G, Li M-X, Zhan Y-G. Numerical study for buckling of pile with different distributions of lateral subgrade reaction. Electronic Journal of Geotechnical Engineering 2014;19 A.

[21] Erbrich CT, Barbour R, Barbosa-Cruz E. Soil-pile interaction during extrusion of an initially deformed pile. Frontiers in Offshore Geotechnics II 2011:489–94. doi:doi:10.1201/b10132-62 10.1201/b10132-62.

[22] Feng G, Ling W, Zhan Y. Numerical Eigenvalue Buckling Analysis of Partially Embedded Piles. The Electronic Journal of Geotechnical Engineering 2013;18:2595–603.

[23] Jesmani M, Nabavi SH, Kamalzare M. Numerical Analysis of Buckling Behavior of Concrete Piles Under Axial Load Embedded in Sand. Arabian Journal for Science and Engineering 2014;39:2683–93. doi:10.1007/s13369-014-0970-5.

[24] Kirsch F, Kortsch P, Richter T, Schädlich B. Bodenmechanische Aspekte bei der Ermittlung der Ramm- schädigung und der Gefahr von Beulerscheinungen. In: Stahlmann J, editor. Fachseminar: Stahl im Wasserbau, Mitteilungen des Instituts für Grundbau und Bodenmechanik der TU Braunschweig. Nr. 100, Braunschweig, Germany: 2015, p. 133–52.

[25] Bakroon M, Daryaei R, Aubram D, Rackwitz F. Arbitrary Lagrangian-Eulerian Finite Element Formulations Applied to Geotechnical Problems. In: Grabe J, editor. Numerical Methods in Geotechnics, Hamburg, Germany: BuK! Breitschuh & Kock GmbH; 2017, p. 33–44. doi:978-3-936310-43-6.

[26] Aubram D, Rackwitz F, Wriggers P, Savidis SA. An ALE method for penetration into sand utilizing optimization-based mesh motion. Computers and Geotechnics 2015;65:241–9. doi:10.1016/j.compgeo.2014.12.012.

[27] Bakroon M, Aubram D, Rackwitz F. Geotechnical large deformation numerical analysis using implicit and explicit integration. In: Bilsel H, editor. 3rd International Conference on New Advances in Civil Engineering, Helsinki, Finland: 2017, p. 26–36.

[28] Benson DJ. Computational methods in Lagrangian and Eulerian hydrocodes. Computer Methods in Applied Mechanics and Engineering 1992;99:235–394. doi:10.1016/0045-7825(92)90042-I.

[29] Aubram D, Rackwitz F, Savidis SA. Contribution to the non-lagrangian formulation of geotechnical and geomechanical processes. Lecture Notes in Applied and Computational Mechanics, vol. 82, Springer International Publishing; 2017, p. 53–100. doi:10.1007/978-3-319-52590-7_3.

[30] Aubram D. Homogeneous equilibrium model for geomechanical multi-material flow with compressible constituents. Journal of Non-Newtonian Fluid Mechanics 2016;232:88–101. doi:10.1016/j.jnnfm.2016.04.001.

[31] Daryaei R, Eslami A. Settlement evaluation of explosive compaction in saturated sands. Soil Dynamics and Earthquake Engineering 2017;97:241–50. doi:10.1016/j.soildyn.2017.03.015.

[32] Bakroon M, Daryaei R, Aubram D, Rackwitz F. Multi-Material Arbitrary Lagrangian-Eulerian and Coupled Eulerian-Lagrangian methods for large deformation geotechnical problems. In: Fernandes M de M, editor. Numerical Methods in Geotechnical Engineering IX, Volume 1 (NUMGE 2018), Porto, Portugal: CRC Press; 2018, p. 673–81.

[33] Bakroon M, Daryaei R, Aubram D, Rackwitz F. Implementation and Validation of an Advanced Hypoplastic Model for Granular Material Behavior. 15th International LS-DYNA® Users Conference, Detroit, Michigan, USA: LSTC and DYNAmore; 2018, p. 12.

[34] Winslow AM. Equipotential zoning of two-dimensional meshes (UCRL-7312). United States: 1963.

[35] van Leer B. Towards the Ultimate Conservative Difference Scheme, V. A Second-Order Sequel to Godunov's Method. Journal of Computational Physics 1997;135:229–48. doi:10.1006/jcph.1997.5704.

[36] Schweiger HF. Results from numerical benchmark exercises in geotechnics. In: Mestat P, editor. 5th European Conference on Numerical Methods in Geotechnical Engineering (NUMGE 2002), Paris: 2002, p. 305–14.

[37] Jardine R. Review of technical issues relating to foundations and geotechnics for offshore installations in the UKCS. London: 2009.

[38] Nadeem M, Chakraborty T, Matsagar V. Nonlinear Buckling Analysis of Slender Piles with Geometric Imperfections. Journal of Geotechnical and Geoenvironmental Engineering 2015;141:06014014. doi:10.1061/(ASCE)GT.1943-5606.0001189.

[39] MSL Engineering Limited. A study of pile fatigue during driving and in-service and of pile tip integrity 2001:1–92.

[40] Timoshenko SP, Gere J. Theory of elastic stability. 1963. doi:3.

[41] Holeyman A, Peralta P, Charue N. Boulder-soil-pile dynamic interaction. Frontiers in Offshore Geotechnics III, CRC Press; 2015, p. 563–8. doi:10.1201/b18442-72.

[42] Yu F, Yang J. Base Capacity of Open-Ended Steel Pipe Piles in Sand. Journal of Geotechnical and Geoenvironmental Engineering 2012;138:1116–28. doi:10.1061/(ASCE)GT.1943-5606.0000667.

[43] Jardine R, Chow F, Overy R, Standing J. ICP Design Methods for Driven Piles in Sands and Clays. Glasgow: Thomas Telford Ltd; 2005.

[44] Röhner R. Der Einfluss der Gestängelänge auf die Ergebnisse von Rammsondierungen (The influence of rod length on the results of dynamic probing). In German. Shaker Verlag, 2010, (In German).